A Cell-Compatible Conductive Film from a Carbon Nanotube Network Adsorbed on Poly-L-lysine

Debora W. Lin, Christopher J. Bettinger, Joshua P. Ferreira, Clifford L. Wang, and Zhenan Bao*

Department of Chemical Engineering, Stanford University, Stauffer III, 381 North-South Mall, Stanford, California 94035-5025, United States

ABSTRACT Single-walled carbon nanotubes (SWNTs) have shown promise for use in organic electronic applications including thin film transistors, conducting electrodes, and biosensors. Additionally, previous studies found applications for SWNTs in bioelectronic devices, including drug delivery carriers and scaffolds for tissue engineering. There is a current need to rapidly process SWNTs from solution phase to substrates in order to produce device structures that are also biocompatible. Studies have shown the use of surfaces covalently functionalized with primary amines to selectively adsorb semiconducting SWNTs. Here we report the potential of substrates modified with physisorbed polymers as a rapid biomaterials-based approach for the formation of SWNT networks. We hypothesized that rapid surface modification could be accomplished by adsorption of poly-L-lysine (PLL), which is also frequently used in biological applications. We detail a rapid and facile method for depositing SWNTs onto various substrate materials using the amine-rich PLL. Dispersions of SWNTs of different chiralities suspended in *N*-methylpyrrolidinone (NMP) were spin coated onto various PLL-treated substrates. SWNT adsorption and alignment were characterized by atomic force microscopy (AFM) while electrical properties of the network were characterized by 2-terminal resistance measurements. Additionally, we investigated the relative chirality of the SWNT networks by micro-Raman spectroscopy. The SWNT surface density was strongly dependent upon the adsorbed concentration of PLL on the surface. SWNT adsorbed on PLL-treated substrates exhibited enhanced biocompatibility compared to SWNT networks fabricated using alternative methods such as drop casting. These results suggest that PLL films can promote formation of biocompatible SWNT networks for potential biomedical applications.

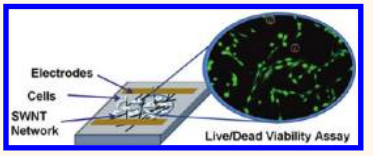

KEYWORDS: single-walled carbon nanotube · poly-L-lysine · biocompatibility

Single-walled carbon nanotubes (SWNTs) exhibit a wide range of unique electrical, mechanical, and chemical properties. Thus they have shown promise for use in organic electronic applications including thin film transistors, conducting electrodes, and biosensors.[1−3] Recently, SWNTs have also attracted interest in applications in biotechnology due to their exceptional electronic properties and functionalizable surfaces.[4−6] In recent years, researchers have begun using SWNTs in bioelectronic devices, as drug delivery carriers of proteins and therapeutic agents,[7−9] and even scaffolds for tissue engineering.[10−12] Several studies investigated the biocompatibility of nanoparticle and carbon nanotube interfaces in several kinds of mammalian cell lines.[13−15] Recent investigations have examined the biocompatibility of nanomaterials with neural tissues and the development of electrodes to electrically stimulate neural cells.[16] Harris *et al*. demonstrated a functional neural interface with microelectrodes composed of multiwalled carbon nanotubes (MWNTs).[4] The ability of the microelectrodes to operate with capacitive current suggests that they can be used without electrochemical hazards and potentially be both efficacious and provide safe electrical stimulation of neurons. Furthermore, Kotov *et al*. investigated the benefits of a carbon nanotube/laminin composite as a neural interface.[6] The composite film successfully served as a platform for the differentiation and electrical stimulation of neural stem cells. Thus far, research on interfacing SWNTs and other nanomaterials with cells and the compatibility of the two have been investigated. A current issue that hinders the advancement of these neural interfaces is the cytotoxicity of the materials used to compose these interfaces. Geckeler *et al*. investigated the cytotoxicity of solution-based functionalized SWNTs when exposed to various mammalian cell lines.[13] They compiled immense information on *in vitro* cytotoxicity results of various types of carbon nanotubes against several kinds of mammalian cell lines.[13] They found that the cytotoxicity was affected by a combination of SWNT aspect ratio (diameter and length), surface area, surface chemistry, aggregation, and purity, making it hard to conclude. Other efforts have investigated the feasibility of chemically modifying SWNTs with biological molecules,[17] while others have observed reduced cytotoxicity of chemically modified

* Address correspondence to zbao@stanford.edu.

Received for review October 7, 2011 and accepted November 4, 2011.

Published online November 04, 2011
10.1021/nn203870c

© 2011 American Chemical Society

MWNTs.[18,19] However, chemically modifying SWNTs or MWNTs often require several steps to ensure specific protein nanotube binding;[17] furthermore, fewer have carried out biocompatibility studies of carbon nanotube networks on substrates. Thus, in this paper we introduce a facile method to improve biocompatibility of carbon nanotube films adsorbed by a polymer treatment of the substrate surface.

In terms of SWNT film deposition, previous studies were able to adsorb SWNTs by drop casting,[20] airbrush spray coating,[21] vacuum filtration,[22] electrophoretic deposition,[23] and Langmuir–Blodgett deposition.[24] The use of surfaces covalently functionalized with primary amines has been shown to selectively adsorb SWNTs.[25,26] Under certain conditions, semiconducting SWNTs can be selectively enriched on amine surfaces.[3,26,27] While others have investigated the biocompatibility of cells and SWNT/MWNT networks formed using APTES surfaces.[28] We hypothesized that amine-SWNT interactions could be extended to biopolymers containing amine moieties to allow both adsorption of SWNTs and biocompatibility. The use of polycationic natural biopolymers could improve the biocompatibility profile of SWNT substrates. We herein report a method to quickly and easily prepare conductive films based on SWNTs adsorbed on PLL surfaces. PLL is a polycationic homopolymer of the naturally occurring peptide L-lysine. It is typically used as an attachment factor to cover tissue culture plates to improve cell adherency.[29] Electrostatic interactions between PLL and plasma treated oxides[30] or plastics promote physisorption of PLL onto substrates and creates a surface that enhances SWNT adsorption. In this work, we describe a rapid and facile method for depositing SWNTs onto various substrate materials using amine-rich biocompatible PLL. We found that PLL treated substrates not only provide an effective method of depositing a carbon nanotube network onto the surface but also exhibited biocompatibility with biological cells.

RESULTS AND DISCUSSION

Film Preparation and Characterization of Substrates. Cell compatible conductive substrates were fabricated in a stepwise fashion. First, we investigated the versatility of PLL to be used as an adhesion layer for adsorption of a carbon nanotube network. The presence of adsorbed PLL films was inferred from the presence of a peak at 398 eV in the high resolution X-ray photoelectron spectroscopy (XPS) spectra of the N1s binding energy region (Figure 1). Water-in-air contact angle measurements of substrates were uniformly reduced upon adsorption of PLL layers. This trend was observed across substrate materials including silicon, glass, and polyethylene terephthalate (PET). For all three types of surfaces that were treated with PLL, we consistently saw that the addition of PLL yielded a decrease in contact angle. For example, glass substrate contact

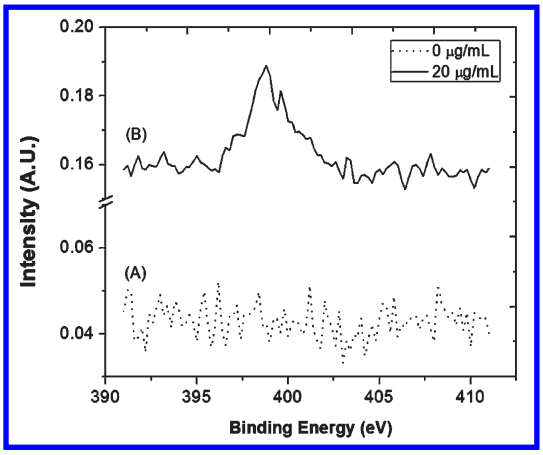

Figure 1. XPS characterization. High resolution XPS spectra of the N1s binding energy region of a control sample without PLL treatment. XPS spectra comparing samples with and without PLL treatment: bottom (A) is control sample; top scan (B) with 20 μg/mL PLL treatment.

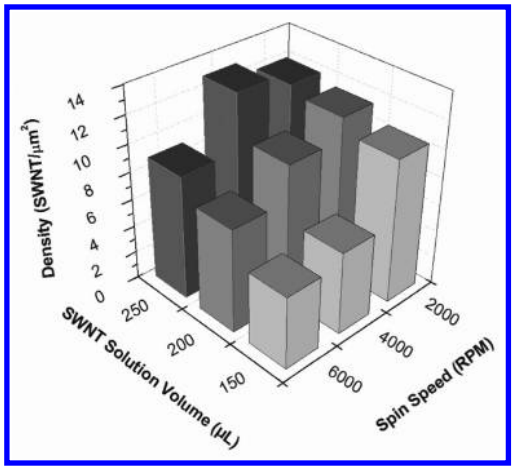

Figure 2. Surface density of SWNT as a function of common processing parameters.

angles decreased from 23.75° ± 0.73° to 17.25° ± 3.3°, which may be explained by the polar side groups on the PLL molecule.

The density of SWNT adsorbed to the surface could be tuned by altering the following deposition parameters: spin speed, volume of solution dispensed, and SWNT solution concentration (Figure 2). A SWNT density of 13 SWNT/μm^2 was obtained by spin coating 250 μL of 5 μg/mL SWNT solution at 4000 rpm, while a density of 5.25 SWNT/μm^2 was obtained by spin coating 150 μL of 5 μg/mL SWNT solution at 6000 rpm. Devices composed with these parameters contained percolating random networks of SWNTs much higher than the percolation threshold. The percolating threshold can be calculated using $\rho_s L_s^2 \gg 4.2362/\pi$, where ρ_s is the number of SWNTs in unit area and L_s is the length of the SWNT.[31] The percolating threshold for the highest density surfaces was calculated to be 13 SWNT/μm^2 or higher based on the length of the SWNT of 1 μm or longer. In comparison, another facile

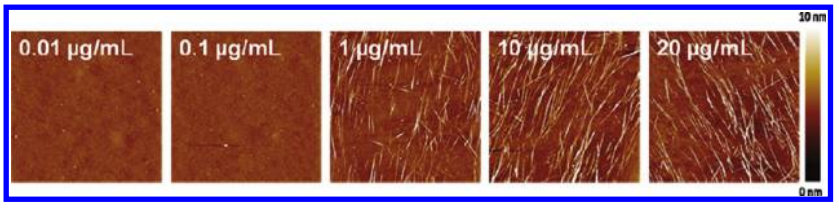

Figure 3. AFM topological micrographs. AFM images of PLL treated spin-coated SWNTs substrates of varying concentration of PLL: 400 μL of SWNT solution was deposited onto each of these substrates. Images are 5 $\times$ 5 μm.

approach to form controllable arrays of SWNT networks involved treating substrates with 3-aminopropyltriethoxysilane (APTES) surface modification to form amine-terminated self-assembled monolayers.[25] Under appropriate pH and spin-coating parameters a SWNT density as high as 20.8 $\pm$ 2.4 SWNT/μm^2 was obtained.[26] In addition, varying PLL concentration was also investigated to control SWNT density (Figure 3). SWNT adsorption was observed to increase with increased PLL concentrations. This effect reached saturation at a PLL concentration of 20 μg/mL. Additionally, it was found that SWNT solutions spin coated onto substrates gave rise to partially aligned networks of SWNTs. SWNTs that are perfectly aligned, where 100% of the SWNTs are aligned within an arbitrary axis, are not ideal because it would not result in a connecting conductive network.

Electronic Properties of SWNT Networks. The ensemble electronic conductivity of spin-coated SWNT networks was directly impacted by both surface preparation and deposition conditions (Figure 4). The conductivity of SWNT networks is increased as the concentration of PLL deposition solutions is increased (Figure 4A), which can likely be attributed to an increase in SWNT density. Increasing SWNT solution concentration also leads to increased SWNT surface density and subsequent enhancements in conductivity (Figure 4B). In subtle contrast to previous studies, SWNT networks adsorbed to amine-containing PLL films exhibited no chiral specificity as determined by Raman spectroscopy (Figure 5).[25] Potential enrichment in semiconducting SWNTs with PLL treated surface was determined through micro-Raman spectroscopy (Figure 5). Using two excitation energies 1.96 and 1.58 eV, micro-Raman spectra showing radial breathing modes found that with varying PLL concentration, neither the semiconducting or metallic peak became enhanced concluding that there is no sorting of SWNTs. This observation is consistent with the previous studies of SWNT adsorption on to primary amine functionalized surfaces treated with buffer solutions of different pH values.[26] It was found that the amine surfaces immersed in an acidic solution of pH 3 showed no selectivity for either semiconducting or metallic SWNTs.[26]

Biocompatibility of SWNT Networks. The use of PLL as a means to adsorb SWNTs onto a surface provides a potential biocompatible platform for biological uses.

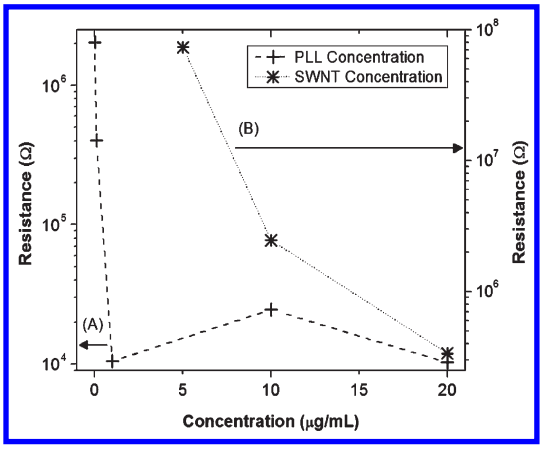

Figure 4. Resistivity measurements of spin-coated SWNT networks. The effect of PLL concentration (A) and SWNT solution concentration (B) on electrical resistance of the SWNT network. Substrates treated with varying PLL concentrations were all spin coated with 400 μL of SWNT solution as shown in Figure 3. Substrates treated with varying SWNT concentration were all treated with the same concentration of PLL (10 μg/mL) and same volume of SWNT solution (400 μL) but different concentrations of the SWNT solution.

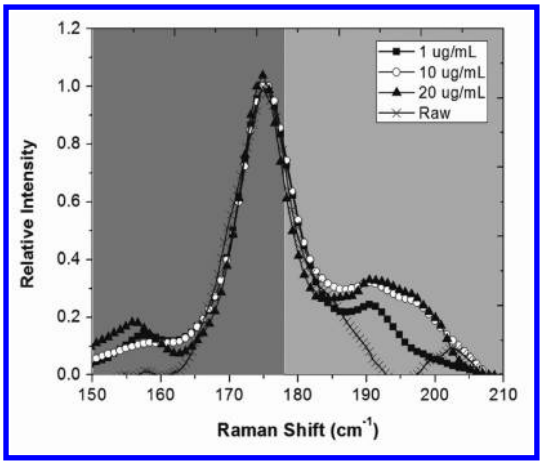

Figure 5. Micro-Raman spectroscopy of SWNT surfaces.

To investigate the biocompatibility of such a hybrid SWNT-PLL substrate, cell morphology (or the shape of the cell) and cytotoxicity studies were conducted. Cellular morphology is an accurate indicator of cell metabolism and viability.[32] Cell morphology was characterized through optical and scanning electron microscopy (SEM). The three conditions tested consisted of PLL-treated glass substrates utilizing two SWNT

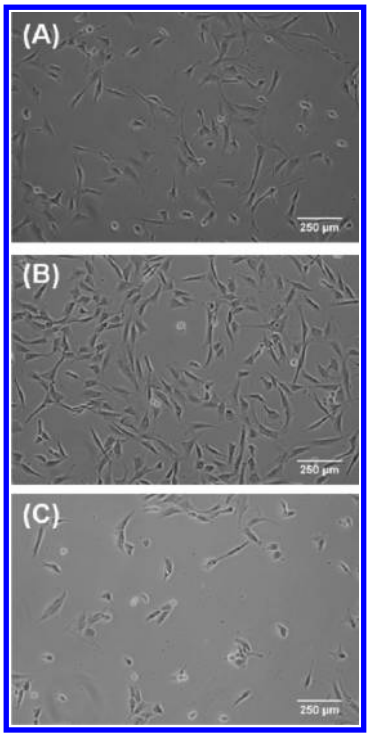

Figure 6. Light microscope images. Morphological changes can be seen between the PLL control (A), spin-coat SWNTs (B), and drop cast SWNTs (C).

deposition techniques and a control without any SWNTs. NIH/3T3 fibroblasts cultured on spin-coated SWNTs PLL-treated substrates adopted more well-spread morphology as compared to drop cast SWNTs PLL-treated slides. On drop cast SWNT/PLL-treated slides, cells contained a more circular morphology suggesting very little growth of protrusive subcellular features[33] as seen in Figure 6. Protruding features such as filopodia are stable when encountered with favorable topological/chemical cues,[33] the lack of these filopodia suggests that the drop cast SWNTs PLL-treated substrates presented an unfavorable topological surface for the cells. SEM micrographs also support light micrograph results. High resolution images in Figure 7 show features extending from the cells on spin-cast SWNTs substrates while drop-coated substrates contained cells that appeared apoptotic. Additionally, it was observed that the cells did not exhibit preferential growth in the direction of SWNT alignment on the spin-coated substrates, suggesting that alignment may not affect cytotoxicity of the SWNTs.

Cytotoxicity of Carbon Nanotubes. In addition to the above cell morphology study, we used two different cytotoxicity studies to observe the effects of the components of the device on cells both quantitatively through mitochondrial activity and qualitatively through fluorescence imaging. The XTT assay was used to monitor the degree of cytotoxicity caused by components of the substrate. In the assay, 400 μL of a 1 mg/mL solution of sodium salt of XTT (2,3-bis[2-methoxy-4-nitro-5-sulfophenyl]-2*H*-tetrazolium-5-carboxyanilide

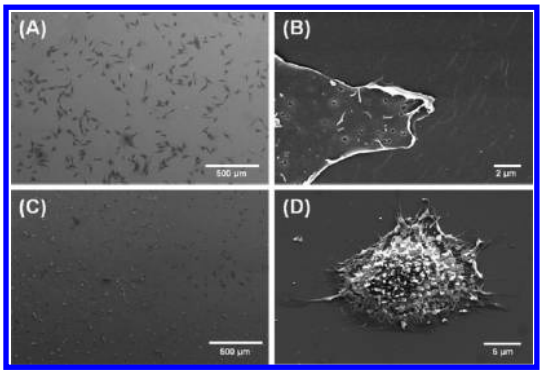

Figure 7. SEM micrographs of spin-coated (A,B) and drop-cast (C,D) substrates and cells.

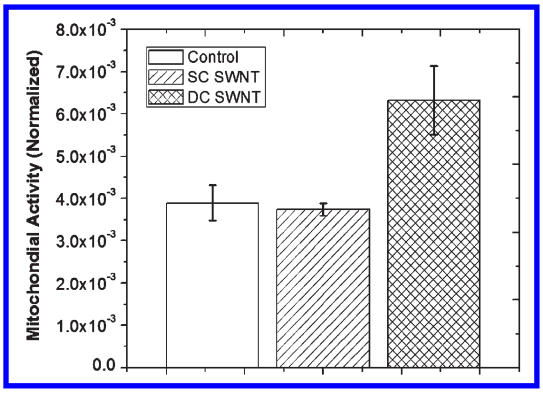

Figure 8. Mitochondrial activity. Effect of spin-coat (SC) SWNT or drop-cast (DC) SWNT on mitochondrial activity.

inner salt) reconstituted in the medium was added to a six-well plate that contained substrates that had cells seeded onto it for 24 h. Three types of substrates were tested, substrates that contained no SWNTs (control), spin-coated SWNTs, and drop-cast SWNTs.

It was found that the mitochondrial activity increased for drop-cast samples when compared to both the control and spin-coated samples when normalized to cell concentration (Figure 8). The increase in mitochondrial activity suggests that drop-cast SWNT induce a more intense toxic response than samples where SWNTs were spin coated or no SWNT at all. These findings may be explained by the orientation of the SWNT on the surface. For drop-cast samples, the SWNT were observed lying on top of each other randomly as compared to spin-coated samples where a partially aligned monolayer of SWNTs was on the surface. Because of the higher roughness of the drop-cast SWNTs, the cell may have had more contact with the SWNT than the surface, thus stronger interactions with the cellular membranes was expected. Similarly, Holt *et al.* investigated the effects of purified and dispersed SWNTs and observed the accumulation of these nanomaterials in the cells and the disruption of cellular processes, such as reduction in cell proliferation and alterations of actin structures.[33]

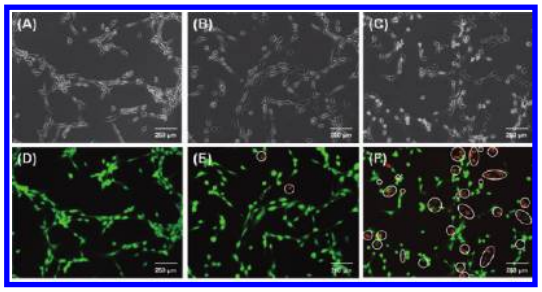

Figure 9. Live/dead assay microscope images. Transmission microscope images (A−C) and fluorescent images (D−F). (A,D) PLL control; (B,E) spin-coat SWNTs substrate; (C,F) drop-cast SWNTs substrate. Live cells fluoresce green and dead cells fluoresce red (emphasized by circles).

The cytotoxicity of carbon nanotubes deposited substrates and 3T3 fibroblasts were also tested by fluorescence staining with live/dead viability/cytotoxicity assay from Molecular Probes. This is a common technique used to fluorescently tag two probes that are frequently characterized parameters of cell viability, intracellular esterase activity, and plasma membrane integrity. Two dyes were used, a cell-permeant calcein AM and EthD-1, which can only enter cells with damaged membranes. When the polyanionic dye calcein enters the cell it is enzymatically converted by intracellular esterase activity into a highly fluorescent calcein producing an intense uniform green fluorescence in live cells. EthD-1 can only enter cells with damaged membranes and becomes highly fluorescent when bound to nucleic acids, thus producing a bright red fluorescence in dead cells. Therefore, cells which have died that contain compromised membranes will contain a bright red florescence, and those that are living and contain intracellular esterase activity will fluoresce bright green. After 24 h of exposure to the different SWNT substrates the cells were stained and confocal live/dead assay images demonstrated that the drop-cast samples had many more dead cells than the spin-coated samples (Figure 9). This suggested that the drop-cast SWNT substrates demonstrated higher cytotoxicity than SWNTs that were spin coated onto the substrate. The data were quantified by taking the ratio of the number of dead cells to the total number of cells for each of the three conditions, control, spin-coat, and drop-cast samples (n = 8). The percentage of dead cells for each condition was calculated to be 0.23%, 3.36%, and 34.37% for the control, spin-coat, and drop-cast samples, respectively. The differences between the percentages for the spin-coat and drop-cast samples were found to be statistically significant using a t test ($p < 0.001$).

Min *et al.* studied the biological behaviors of NIH-3T3 fibroblasts on graphene and MWNTs composite artificial surfaces. Their study suggested that the nanomaterials show high biocompatibility for bioapplications based on their results on proliferation, focal adhesion, and gene transfection studies.[28] Our results here show that spin assembly of a low-roughness SWNT network on a biocompatible PLL surface is an effective way to prepare

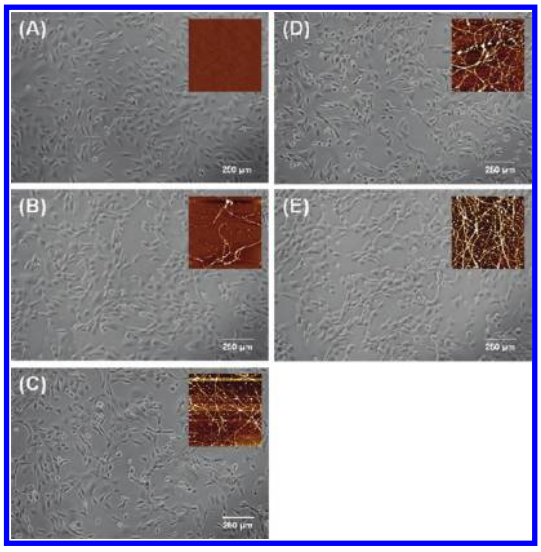

Figure 10. Light microscope images. Morphological changes can be seen between the control (A), 30 spray-coated layers (B), 50 spray-coated layers (C), 70 spray-coated layers (D), 90 spray-coated layers (E). Insets are corresponding AFM images, 5 μm.

conductive substrates compatible with cells. In contrast, high-roughness SWNT films formed by drop casting led to cell death. Our biocompatible conductive surfaces can be useful for devices that require cell-SWNT contact such as neural interfaces that involve electrical stimulation of cells and devices that utilize sensing mechanisms based on the interactions of the mechanical forces of the cells and their interaction with the SWNT network.

To further elucidate the effect of SWNT roughness on biocompatibility, cell morphology was observed on substrate surfaces of varying SWNT network density. These samples were treated with PLL and deposited with SWNT solution using a spray coating method. The spray coating method was used to create a broader range of SWNT network densities. To vary the SWNT network density, the number of sprays differed between samples 30, 50, 70, and 90 sprays. It was observed that as the SWNT density increased, so did the number of cells that depicted circular morphology, which is an indication of an unfavorable topological surface for the cells as previously discussed, shown in Figure 10. Furthermore, the percentage of dead cells for each condition was calculated to be 8.02%, 6.12%, 25.64%, and 18.98% for the 30, 50, 70, and 90 sprays, respectively. For sprayed SWNT networks with the same density as the spin-coated SWNT film, the main difference is the roughness of the films, calculated using the root-mean-square. Films created from spray coating or drop-cast methods contained roughness greater than 6 nm and heights of SWNTs in the range of 5−30 nm. Films on spin-coated substrates contained surface roughness values of under 2 nm and SWNT heights in the range of 1−5 nm. These results indicate that roughness of the SWNT film is an important factor to consider, suggesting that spin-coated uniform

SWNT films provide the most biocompatible surface for cells.

CONCLUSION

We demonstrate reduced toxicity of SWNT networks processed on surfaces functionalized with PLL. PLL, commonly used to promote cell adhesion, also provides a rapid and facile method for depositing SWNTs onto various substrate materials. Increasing the concentration of PLL and SWNT solution leads to networks with increased densities and order of magnitude reductions in sheet resistance. Light microscopy and SEM demonstrate healthy elongated cell morphology on spin-coated SWNT surfaces *versus* circular cell morphology on drop-cast devices. Furthermore, XTT assay shows that mitochondrial activity on spin-coated smooth SWNT networks maintained similar levels as the control, justifying that such a SWNT morphology presents biocompatibility and conductivity simultaneously. In addition, live/dead assays showed increased cytotoxicity with SWNT networks that have been deposited by drop-cast methods *versus* spin-coated methods. This work represents a simple approach to improve biocompatibility of SWNT networks for the development of conductive surfaces for biomedical applications.

METHODS

Preparation of Substrates. Heavily doped silicon wafers (Silicon Quest, Santa Clara, CA, USA, 100 orientation with 300 nm thermal oxide) and glass substrates were sectioned into 25 mm × 25 mm squares. Substrates were solvent rinsed in acetone, isopropyl alcohol, methanol, and water and dried in an N_2 stream. Substrates were ozone cleaned for 10 min (UVO Cleaner, Jelight Company Inc.) and incubated in a 10 μg/mL poly-L-lysine solution (Sigma-Aldrich) for 1 h.

Purification of SWNTs. Dilute SWNT solutions were prepared using a modification of a previous procedure.[26] An 80 mg portion of arc-discharge single walled nanotubes (AD-SWNTs) obtained from ILJIN Nanotech, grade ASP-100F and 2 g of sodium dodecyl sulfate (SDS), from J. T. Baker were mixed with 200 mL of ultrapure water (0.1 micro-filtered, Invitrogen). The mixture was sonicated (Cole-Parmer Ultrasonic Processor) at 750 W, 100% amplitude for 30 min with ice-water bath and then centrifuged (Sorvall RC5C Plus) at 12500 rpm for 4 h at 4 °C. The supernatant (~80%) was decanted and diluted with anhydrous acetone, the surfactant (SDS) was dissociated from SWNTs and the flocculated SWNTs were collected by centrifugation. Upon washing the flocculated SWNTs with acetone several times to completely remove the surfactant, the suspension was filtered through PTFE membrane (Millipore, 0.45 μm pore size) to collect the nanotubes. Macroscopic SWNT film was peeled off from the membrane and dried under vacuum at 50 °C overnight.

Nanotube Solution Preparation. Nanotube solution was prepared from the purified macroscopic SWNT film by sonicating the bucky paper in NMP (1-methyl-2-pyrrolidone, Omnisolve, spectrophotometry grade) for 25 min to final concentrations of 5, 10, and 20 μg/mL.

Preparation of Spin-Coat, Drop-Cast, and Spray-Coat Samples. For spin-coat samples, nanotube solutions were deposited dropwise on newly cleaned substrates. For biocompatibility studies, drop-casted samples were prepared by depositing 400 μL of nanotube solution directly on the substrate and were dried at 120 °C for 2 h under vacuum. To prepare spray-coated samples, SWNTs were spray-coated from solution using a commercial airbrush (Master Airbrush, model SB844-SET). The substrates were held at 180 °C on a hot plate, and the SWNTs were sprayed at a distance of approximately 4 in. using an airbrush pressure of 35 psi. The samples were then dried at 90 °C for 30 min under vacuum. PLL was adsorbed to various substrates including native silicon oxide and glass slides using aqueous solutions of the polyamino acid.

Sample Characterization and Imaging. XPS analysis was performed on a PHI 5000 Versaprobe equipped with an Al kα X-ray source. High-resolution spectra were collected at a takeoff angle of 45°, a pass energy of 23.5 eV and a step size of 0.1 eV. Atomic force microscopy (AFM) topography images were acquired in the tapping mode regime using a Multimode AFM (Veeco). Scanning electron microscope images were acquired using a variable pressure SEM (Hitachi S-3400N VP-SEM, Pleasanton, CA) and high pressure SEM (FEI XL30 Sirion, Hillsboro, Oregon). Fluorescent microscope images were acquired using an inverted light microscope (Zeiss Axio Observer Z1, Thornwood, NY). Electrical characterization of the devices was carried out using a parameter analyzer, Keithley 4200 SC semiconductor analyzer, to measure the resistance of the SWNT network.

Cell Viability. NIH-3T3 mouse fibroblasts were used to investigate the biocompatibility of the conductive SWNT/PLL film. NIH-3T3 cells are commonly used in cell studies that investigate cell morphology, proliferation, and adhesion.

XTT Assay. A 400 μL aliquot of a 1 mg/mL solution of sodium salt of XTT (2,3-bis[2-methoxy-4-nitro-5-sulfophenyl]-2*H*-tetrazolium-5-carboxyanilide inner salt) reconstituted in the medium was added a six-well plate that contained substrates that had 3T3 cells seeded onto for 24 h. The assay was then incubated at 37 °C for 4 h. Absorbances were measured at 450 and 690 nm values. Absorbances taken at 690 nm served as the background measurement and were subtracted from the 450 nm value.

Live/Dead Viability/Cytotoxicity Assays. Live/dead viability/cytotoxicity assays were performed according to manufacturer's instructions (Molecular Probes). Briefly, 20 μL of the 2 mM EthD-1 stock solution was added to 10 mL of sterile, tissue culture, grade D-PBS to make a 4 μM EthD-1 solution. Five μL of the 4 mM calcein AM stock solution was then added to 10 mL of EthD-1 solution. The working solution comprising both calcein AM and EthD-1 was added directly to the 3T3 cells. Cells were then incubated for 45 min at room temperature. Labeled cells were then viewed and pictured under the fluorescence microscope.

Acknowledgment. The authors thank W. Overton, R. Peacock, and J. Vroom for their helpful discussions and suggestions. The authors also thank R. Stoltenberg for the assistance with XPS and SEM analysis. D.W.L. was supported by the National Defense Science and Engineering Graduate (NDSEG) Fellowship, 32 CFR 168a and the National Science Foundation Graduate Research Fellowship. C.J.B. was supported by a Ruth L. Kirschstein Fellowship (Grant No. 1F32NS064771).

REFERENCES AND NOTES

1. Tasca, F.; Zafar, M. N.; Harreither, W.; Ludwig, R.; Noll, G. A Third Generation Glucose Biosensor Based on Cellobiose Dehydrogenase from *Corynascus Thermophilus* and Single-Walled Carbon Nanotubes. *Analyst* **2010**, 2033–2036.
2. Xu, X.; Jiang, S.; Hu, Z.; Liu, S. Nitrogen-Doped Carbon Nanotubes: High Electrocatalytic Activity toward the Oxidation of Hydrogen Peroxide and Its Application for Biosensing. *ACS Nano* **2010**, *4*, 4292–4298.
3. Roberts, M. E.; LeMieux, M. C.; Sokolov, A. N.; Bao, Z. Self-Sorted Nanotube Networks on Polymer Dielectrics for Low-Voltage Thin-Film Transistors. *Nano Lett* **2009**, *9*, 2526–2531.

4. Wang, K.; Fishman, H. A.; Dai, H.; Harris, J. S. Neural Stimulation with a Carbon Nanotube Microelectrode Array. *Nano Lett.* **2006**, *6*, 2043–2048.
5. Voelker, M.; Fromherz, P. Signal Transmission from Individual Mammalian Nerve Cell to Field-Effect Transistor. *Small* **2005**, *1*, 206–210.
6. Kam, N. W. S.; Jan, E.; Kotov, N. A. Electrical Stimulation of Neural Stem Cells Mediated by Humanized Carbon Nanotube Composite Made with Extracellular Matrix Protein. *Nano Lett.* **2009**, *9*, 273–278.
7. Degim, I. T.; Burgess, D. J.; Papadimitrakopoulos, F. Carbon Nanotubes for Transdermal Drug Delivery. *J. Microencapsul.* **2010**, *27*, 669–681.
8. Chaudhuri, P.; Soni, S.; Sengupta, S. Single-Walled Carbon Nanotube-Conjugated Chemotherapy Exhibits Increased Therapeutic Index in Melanoma. *Nanotechnology* **2010**, *21*, 025102.
9. Zhang, X. K.; Meng, L. J.; Lu, Q. H.; Fei, Z. F.; Dyson, P. J. Targeted Delivery and Controlled Release of Doxorubicin to Cancer Cells Using Modified Single Wall Carbon Nanotubes. *Biomaterials* **2009**, *30*, 6041–6047.
10. Tan, W.; Twomey, J.; Guo, D.; Madhavan, K.; Li, M. Evaluation of Nanostructural, Mechanical, and Biological Properties of Collagen-Nanotube Composites. *IEEE Trans. Nanobiosci.* **2010**, *9*, 111–120.
11. Olivas-Armendariz, I.; Garcia-Casillas, P.; Martinez-Sanchez, R.; Martinez-Villafane, A.; Martinez-Perez, C. A. Chitosan/MWCNT Composites Prepared by Thermal Induced Phase Separation. *J. Alloy. Compd.* **2010**, *495*, 592–595.
12. Jang, M. J.; Namgung, S.; Hong, S.; Nam, Y. Directional Neurite Growth Using Carbon Nanotube Patterned Substrates as a Biomimetic Cue. *Nanotechnology* **2010**, *21*, 235102.
13. Lee, Y.; Geckeler, K. E. Carbon Nanotubes in the Biological Interphase: The Relevance of Noncovalence. *Adv. Mater.* **2010**, *22*, 4076–4083.
14. Motskin, M.; Wright, D. M.; Muller, K.; Kyle, N.; Gard, T. G.; Porter, A. E.; Skepper, J. N. Hydroxyapatite Nano and Microparticles: Correlation of Particle Properties with Cytotoxicity and Biostability. *Biomaterials* **2009**, *30*, 3307–3317.
15. Yin, H.; Casey, P. S.; McCall, M. J.; Fenech, M. Effects of Surface Chemistry on Cytotoxicity, Genotoxicity, and the Generation of Reactive Oxygen Species Induced by ZnO Nanoparticles. *Langmuir* **2010**, *26*, 15399–15408.
16. Kotov, N. A.; Winter, J. O.; Clements, I. P.; Jan, E.; Timko, B. P.; Campidelli, S.; Pathak, S.; Mazzatenta, A.; Lieber, C. M.; Prato, M.; *et al*. Nanomaterials for Neural Interfaces. *Adv. Mater.* **2009**, *21*, 3970–4004.
17. Shim, M.; Shi Kam, N. W.; Chen, R. J.; Li, Y.; Dai, H. Functionalization of Carbon Nanotubes for Biocompatibility and Biomolecular Recognition. *Nano Lett.* **2002**, *2*, 285–288.
18. Smart, S. K.; Cassady, A. I.; Lu, G. Q.; Martin, D. J. The Biocompatibility of Carbon Nanotubes. *Carbon* **2006**, *44*, 1034–1047.
19. Hu, H.; Ni, Y.; Montana, V.; Haddon, R. C.; Parpura, V. Chemically Functionalized Carbon Nanotubes as Substrates for Neuronal Growth. *Nano Lett.* **2004**, *4*, 507–511.
20. Kymakis, E.; Amaratunga, G. A. J. Single-Wall Carbon Nanotube/Conjugated Polymer Photovoltaic Devices. *Appl. Phys. Lett.* **2002**, *80*, 112–114.
21. Lehman, J. H.; Engtrakul, C.; Gennett, T.; Dillon, A. C. Single-Wall Carbon Nanotube Coating on a Pyroelectric Detector. *Appl. Opt.* **2005**, *44*, 483–488.
22. Holzinger, M.; Hirsch, A.; Bernier, P.; Duesberg, G. S.; Burghard, M. A New Purification Method for Single-Wall Carbon Nanotubes (SWNTs). *Appl. Phys. A-Mater. Sci. Process.* **2000**, *70*, 599–602.
23. Chunsheng, D.; Heldbrant, D.; Ning, P. Preparation and Preliminary Property Study of Carbon Nanotubes Films by Electrophoretic Deposition. *Mater. Lett.* **2002**, *57*, 434–438.
24. Krstic, V.; Duesberg, G. S.; Muster, J.; Burghard, M.; Roth, S. Langmuir-Blodgett Films of Matrix-Diluted Single-Walled Carbon Nanotubes. *Chem. Mater.* **1998**, *10*, 2338.
25. LeMieux, M. C.; Roberts, M.; Barman, S.; Jin, Y. W.; Kim, J. M.; Bao, Z. Self-Sorted, Aligned Nanotube Networks for Thin-Film Transistors. *Science* **2008**, *321*, 101–104.
26. Opatkiewicz, J. P.; LeMieux, M. C.; Bao, Z. Influence of Electrostatic Interactions on Spin-Assembled Single-Walled Carbon Nanotube Networks on Amine-Functionalized Surfaces. *ACS Nano* **2010**, *4*, 1167–1177.
27. Ju, S. Y.; Utz, M.; Papadimitrakopoulos, F. Enrichment Mechanism of Semiconducting Single-Walled Carbon Nanotubes by Surfactant Amines. *J. Am. Chem. Soc.* **2009**, *131*, 6775–6784.
28. Ryoo, S.-R.; Kim, Y.-K.; Kim, M.-H.; Min, D.-H. Behaviors of NIH-3T3 Fibroblasts on Graphene/Carbon Nanotubes: Proliferation, Focal Adhesion, and Gene Transfection Studies. *ACS Nano* **2010**, *4*, 6587–6598.
29. Cornbrooks, C. (Book review) Methods for Preparation of Media, Supplements, and Substrata for Serum-Free Animal Cell Culture. *Muscle Nerve* **1986**, *1986*, 268–269 (Banes, D.; Sirbsu, D.; Sato, G. Alan, R; Eds.; Liss, Inc.: New York, 1984).
30. Coll Ferrer, M. C.; Yang, S.; Eckmann, D. M.; Composto, R. J. Creating Biomimetic Polymeric Surfaces by Photochemical Attachment and Patterning of Dextran. *Langmuir* **2010**, *26*, 14126–14134.
31. Kocabas, C.; Pimparkar, N.; Yesilyurt, O.; Kang, S. J.; Alam, M. A.; Rogers, J. A. Experimental and Theoretical Studies of Transport through Large Scale, Partially Aligned Arrays of Single-Walled Carbon Nanotubes in Thin Film Type Transistors. *Nano Lett.* **2007**, *7*, 1195–1202.
32. Chen, C. S.; Mrksich, M.; Huang, S.; Whitesides, G. M.; Ingber, D. E. Geometric Control of Cell Life and Death. *Science* **1997**, *276*, 1425–1428.
33. Holt, B. D.; Short, P. A.; Rape, A. D.; Wang, Y.-l.; Islam, M. F.; Dahl, K. N. Carbon Nanotubes Reorganize Actin Structures in Cells and *ex Vivo*. *ACS Nano* **2010**, *4*, 4872–4878.